High-Speed VCSEL Arrays for 400 Gbit/s Data Center Interconnects

Takeshi AOKI*, Ryosuke KUBOTA, Susumu YOSHIMOTO, Masaki YANAGISAWA, Takashi ISHIZUKA, and Hajime SHOJI

This paper reviews device design and performance of high-speed vertical cavity surface emitting laser (VCSEL) arrays for next-generation short-reach 400 Gbit/s applications in data centers using the advanced PAM-4 modulation format. The both 850 nm/900 nm PAM-4 VCSELs have been optimized to improve dynamic performance and suppress noise for PAM-4 transmission. The new VCSELs also show good uniformity of characteristics, which is advantageous for array products.

Keywords: VCSEL, PAM-4, data center, 400 Gbit/s, 850 nm/900 nm

1. Introduction

Driven by the introduction of fifth-generation (5G) mobile network systems and the rapid market growth of emerging technologies such as artificial intelligence (AI), virtual/augmented reality (VR/AR), and Internet of Things (IoT), the data traffic in data centers is continuously increasing. Optical interconnect infrastructures in the data centers have evolved from 100 Gbit/s to the next-generation 400 Gbit/s data rate. Recently, standardization organizations including IEEE have been dedicated to defining specifications for short-reach 400 Gbit/s interconnects,[1] where vertical cavity surface emitting lasers (VCSELs) are employed with necessarily utilizing a PAM-4*[1] modulation format. PAM-4 is a type of multi-level modulation that can double the number of bits in data transmission. Modulating VCSELs with PAM-4 at a modulation rate of 25 Gbaud leads to 50 Gbit/s transmission. The standard solution targeting 400 Gbit/s optical interconnects is integrating more than one 50 Gbit/s VCSEL in parallel. Thus, the 400G-SR8[2] standard requires a 1 × 8 arrayed 850 nm VCSEL, while the 400G-BD4.2[3] standard requires a set of two different wavelengths 1 × 4 VCSEL arrays of 850 nm and 900 nm, employing a bi-directional transmission (BiDi) using a wavelength division multiplexing technique.

In order to meet these market demands, we have developed VCSELs optimized for the 50 Gbit/s PAM-4 operation in a two wavelength lineup (850 nm/900 nm). In this paper, we review the latest device designs and demonstrate key performance. Also shown is good uniformity of device characteristics, which is strongly required for 400 Gbit/s array products.

2. Device Design Considerations

2-1 Requirements for PAM-4 VCSELs

PAM-4 is a multi-level modulation format of signals using four optical intensity levels as bits. The signal modulated by PAM-4 is more complex than that by the conventional modulation format such as non-return-to-zero (NRZ), in which only two optical intensity levels (on/off) are used. The bit error rate of optical transceivers is more sensitive to the dynamic performance of VCSELs. For the PAM-4 signaling, a higher modulation bandwidth with a flatter frequency response is mandatory to suppress inter-symbol interference, along with strict requirements for relative intensity noise (RIN)*[2] to ensure S/N ratios in each levels.[4] Furthermore, a small spectral width is preferred to suppress mode distribution noise in optical fibers over practical distances.[5]

To meet these requirements, we have improved the VCSEL designs for 50 Gbit/s PAM-4 operation (PAM-4 VCSEL) based on our previous 28G bit/s design[6] (28G VCSEL).

2-2 Device structure

Figure 1 represents the schematic cross-section view of our oxide-confined VCSEL. The design is the same for the two wavelengths of 850 nm and 900 nm. The epitaxial layer structures are grown by the metal organic chemical vapor deposition (MOCVD) on a GaAs substrate. The active layer comprises strained InGaAs/AlGaAs multiple quantum wells (MQWs). The active layer and spacers are sandwiched between a top p-doped AlGaAs distributed
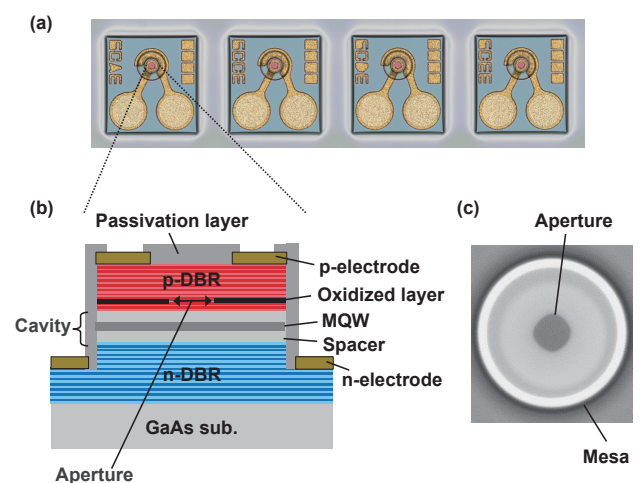

Fig. 1.   (a) Appearance (1 × 4 array), (b) schematic cross-section view, and (c) microscope image of oxide aperture of a VCSEL

Bragg reflectors (DBR) and a bottom n-doped AlGaAs DBR to form an optical cavity in the direction perpendicular to the substrate. The optical length of cavity is designed to have a half of the laser oscillation wavelength to improve the optical confinement of the longitudinal mode and carrier transport. The oxide aperture for current and transverse optical mode confinements are defined by the selective oxidation of a single aluminum-rich AlGaAs layer included in the top DBR just above the active layer. The wet oxidation process is carried out after mesa etching. Dielectric films are formed to protect the surface and tune the optical phase of the top DBR.

2-3 Design for higher bandwidth

The modulation bandwidth of VCSELs is limited by the resonant interactions between the carrier and photon in the stimulated emission process, along with the electrical parasitic components. To realize a high bandwidth, it is particularly important to increase the relaxation oscillation frequency (f_r).[*3] f_r can be written as[7]

$$f_r = D\sqrt{J - J_{th}} \quad\text{.. (1)}$$

where J is the bias current density, J_{th} is the threshold current density, and D is the coefficient (D-factor). While an increase in the current density enhances f_r, it can inevitably shorten the wear-out lifetime of the device. Furthermore, f_r easily reaches the thermal saturation at a high current density because the thermal resistance of VCSELs is higher than that of edge-emitting lasers. Therefore, f_r must increase rapidly even at a low current density. This means that it is important to increase the D-factor. The D-factor is related to an optical confinement factor of the cavity and a differential gain of the MQW. In this paper, we focus on the former factor.

Figure 2 is a schematic illustration of a VCSEL epitaxial layer structure and the optical field distribution of the longitudinal mode. The effective cavity length (L_{eff}) is shown in Fig. 2, which is approximately 1 μm, larger than the nominal cavity length defined as the space between top/bottom DBRs (Cavity in Fig. 2), because the optical field penetrates the top/bottom DBRs to some extent. Here, only the overlapping between MQW and optical field contributes to the interactions between the carrier and photon. Accordingly, when designing an epitaxial layer structure, it
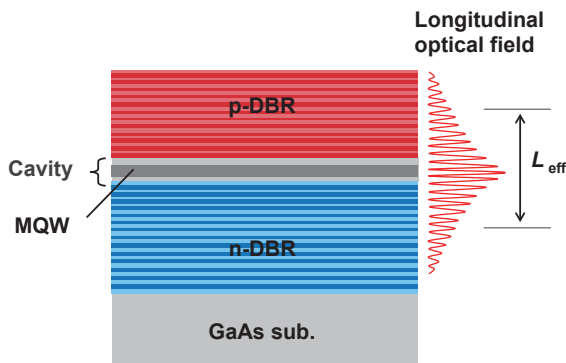
is preferable to minimize the L_{eff} and concentrate light on the MQW in order to enhance a longitudinal optical confinement. In a new epitaxial design, the optical confinement is enhanced by precisely aligning the optical phase of the top/bottom DBRs and the cavity, and by optimizing the standing wave of the resonant cavity. Device simulation including a transient analysis was carried out to examine the impact of epitaxial design on the small signal frequency responses as shown in Fig. 3. Enhancement of optical confinement was expected to increase the bandwidth by about 2 GHz (defined at -3 dB) compared with the conventional design. Thus, this epitaxial layer design was employed for the current PAM-4 VCSEL.
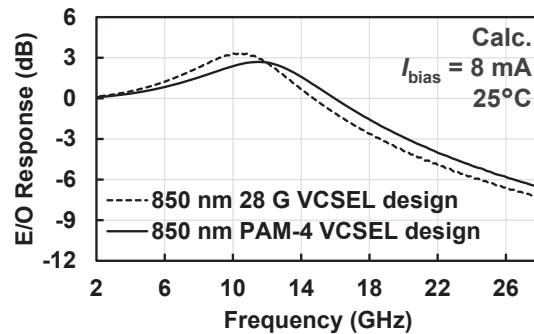

Fig. 3. Simulation of small signal frequency response

To pursue an error-free PAM-4 transmission, an appropriate damping of the frequency response is also important, in addition to the high modulation bandwidth.[8] Figure 4 depicts a damping dependency of the small signal frequency response curves (simulation), exhibiting a resonance peaking when damping is weak. This is undesirable because it causes overshoots in the optical output waveform and fluctuations in the time direction (jitters). Meanwhile, over-damping bends down the curve to suppress the bandwidth. Here, the damping increases in proportion to f_r^2, while it can be controlled by the photon lifetime in the cavity.[7] Accordingly, a key to attaining a high bandwidth along with a flat frequency response is to balance the damping increase resulting from the f_r

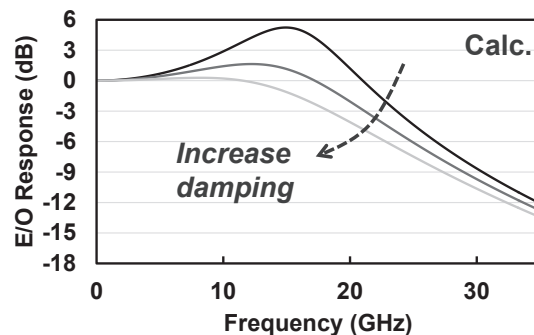Fig. 2. The epitaxial layer structure and optical field distribution

Fig. 4. Impact of damping on resonance peaking in small signal frequency response

enhancement, by adjusting the photon lifetime. For the new PAM-4 VCSEL, we precisely control the phase of the top reflection to optimize the photon lifetime, by tuning the thickness of both top DBR and dielectric film. It should be noted that the optical phase also affects the light output power and threshold current. The trade-off between the characteristics should be taken into account.

2-4 Transverse mode control

The oxide aperture of a VCSEL behaves as an index-guide like a core/clad of an optical fiber, because the refractive index of an oxidized AlGaAs is lower than that of semiconductors. It determines the transverse mode of a VCSEL. Our VCSEL exhibits a multimode lasing behavior of the transverse modes, where the spatial distribution, spectral spacing, and intensity ratio in each transverse mode are important because they have correlation with the lasing spectra and the generation of noise.[9] We optimized the aperture shape to control the transverse mode.[10]

Figure 5 shows the microscope images of rotationally symmetric (circular) and asymmetric apertures, and the calculated optical intensity distribution for the corresponding transverse modes. Typical lasing spectra measured for the respective apertures are shown in Fig. 6. We find out in the spectrum of the circular aperture in (a) that multiple transverse modes are overlapped at almost the same wavelength (peaks 4, 5, and 6 in Fig. 6 (a)). These overlapped transverse modes have spatially different distri-
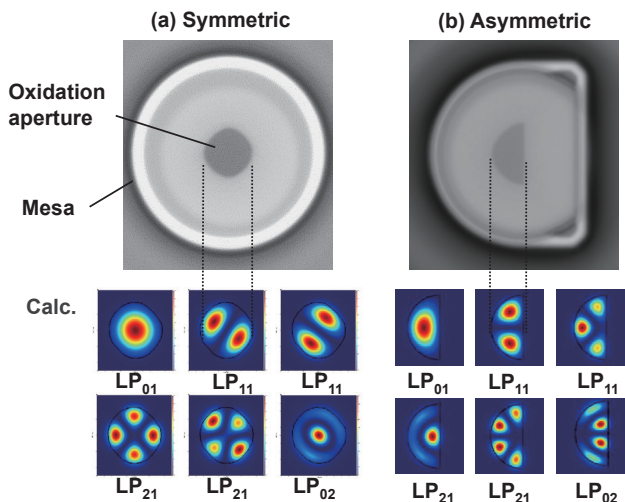
butions of optical intensity but degenerate. The multiple lasing modes in the close wavelengths interact with each other, so that mode transitions occur continuously. This causes spatial fluctuations of light output power, contributing to the generation of noise. Meanwhile, in the spectrum of a rotationally asymmetric aperture (Fig. 5 (b)), the number of peaks increases since the overlapped transverse modes are split and separately distributed (Fig. 6 (b)). In this case, mode transitions could be suppressed, possibly reducing the generation of noise. In addition, the rotational asymmetry of the oxide aperture plays an important role in stabilizing the polarization plane of the VCSEL.[11] This effect can also contribute to the noise reduction. Consequently, we have adopted this rotationally asymmetric aperture design for the PAM-4 VCSELs to reduce the RIN.

3. Device Characterization

3-1 Static performance

Figure 7 shows typical light output power *versus* current (*L-I*) characteristics of 850 nm and 900 nm PAM-4 VCSEL 1 × 4 arrays. The *L-I* curves of the four channels show almost the same characteristics for both wavelengths. At 90°C, the threshold current (I_{th}) is below 0.9 mA, with a slope efficiency (SE) of larger than 0.4 W/A, and an output power of above 2 mW at a bias current of 8 mA. The saturation in optical output due to self-heating is not observed even at a bias current of 10 mA, suggesting that our VCSELs have good temperature characteristics.
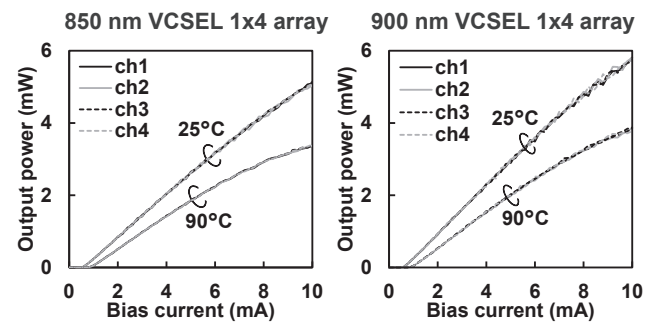

Fig. 5. Transverse modes of rotationally symmetric/asymmetric apertures

Fig. 7. Light output power vs. bias current characteristics

Fig. 6. Lasing spectra of rotationally symmetric / asymmetric apertures

Typical root-mean-square spectral width of the 850 nm VCSEL at a bias current of 8 mA is 0.35 nm at 25°C and 0.24 nm at 90°C. The 900 nm VCSEL shows the typical spectral width of 0.55 nm at 25°C and 0.39 nm at 90°C. These values meet the requirement in IEEE P802.3cm proposal (less than 0.6 nm at 850 nm, and 0.65 nm at 900 nm).[5] RIN is estimated from the average and deviation of light output power measured using a digital communication analyzer (DCA) with a fixed bias condition at 8 mA. The typical RIN values are −142.2 dB/Hz for 850 nm VCSEL and −142.8 dB/Hz for the 900 nm VCSEL. These values satisfied the criteria for PAM-4 transmission

proposed by Tatum et al.[12] (below −138 dB/Hz). RIN values were reduced by approximately 4 dB/Hz from that of our 28G VCSEL, due to the modified transverse mode by utilizing a rotationally asymmetric aperture as discussed above.

3-2 Dynamic performance

Figure 8 shows the typical small signal frequency response of the 850 nm and 900 nm PAM-4 VCSELs. The 3 dB bandwidth exceeds 18.5 GHz at room temperature for both VCSELs. The high bandwidth is maintained at above 17 GHz even at 90°C. We improved the bandwidth by 2 GHz or more compared with the 28G VCSEL, due to the f_r enhancement by carefully tuning the epitaxial layer structure, as discussed above. The height of resonance peaking in the frequency response was suppressed to less than 3 dB even at 90°C, as a result of appropriate adjustment of damping by controlling the photon lifetime.

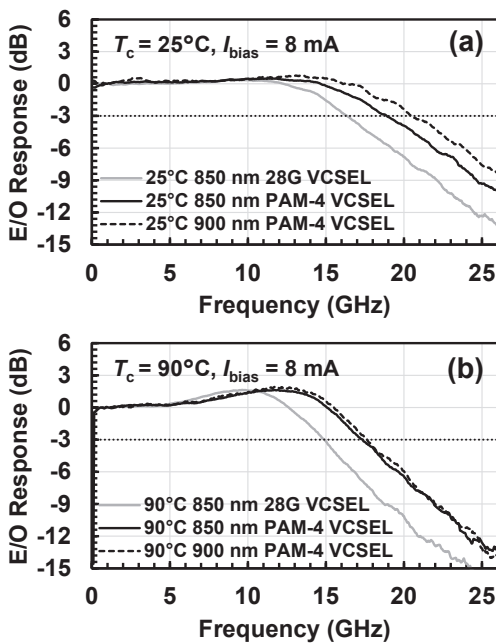Fig. 9. PAM-4 optical output waveform (eye diagram)

Fig. 8. Small-signal frequency response

Figure 9 shows the optical output waveform of the PAM-4 modulation (eye diagram) with a bias current of 8 mA at 25°C and 90°C, for both the 850 nm/900 nm PAM-4 VCSELs. An arbitrary waveform generator (AWG) and a high-frequency probe are used to input PAM-4 signals of 25.5625 Gbaud (51.125 Gbit/s). The optical output of the VCSEL was measured using a sampling oscilloscope.

Overshoots and jitters are well-suppressed at each of the four intensity levels in the PAM-4 waveform, and clear eye-patterns are confirmed. TDECQ,[*4] which is a figure-of-merit of the PAM-4 waveform, is less than 3 dB even at a high temperature (90°C), and meets the requirement of the IEEE P802.3cm (less than 4.5 dB).[13] The high quality waveforms are achieved with the combination of a high bandwidth exceeding 17 GHz, flat frequency response, and low RIN, as discussed above. Thus, we demonstrated that
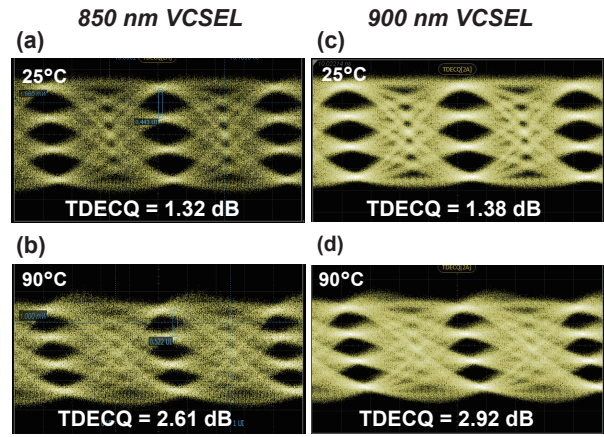
our VCSEL is suitable to the PAM-4 modulation, enabling transmission at over 50 Gbit/s for both wavelengths.

3-3 Uniformity of characteristics

The 1 × 4 or 1 × 8 VCSEL array products for 400 Gbit/s applications are configured with several VCSEL chips that are adjacent to each other on the same wafer. To improve the production yield, the array product needs to have a higher level of uniformity in characteristics than a single chip product. The light output power and bandwidth uniformity are highly related to the qualities of MOCVD growth and subsequent device fabrication processes, which are already at high levels due to the matured manufacturing experiences. Meanwhile, the spectral width and RIN still have a certain amount of variations, because they are related to an inevitable random distribution of aperture shapes.

Figure 10 presents the box plots of the root-mean-square spectral width and RIN for 850 nm VCSELs as an example. It shows that variations in the spectral width and RIN of the PAM-4 VCSEL are much smaller than those of the 28G VCSEL. This suggests that our new design offers the robust characteristics against the structural variation, attributed to the stabilized transverse mode by employing the rotationally asymmetric oxide aperture instead of conventional circular aperture as discussed above. As a result, with low variations in the spectral width and RIN, our PAM-4 VCSEL achieves high uniformity in all charac-
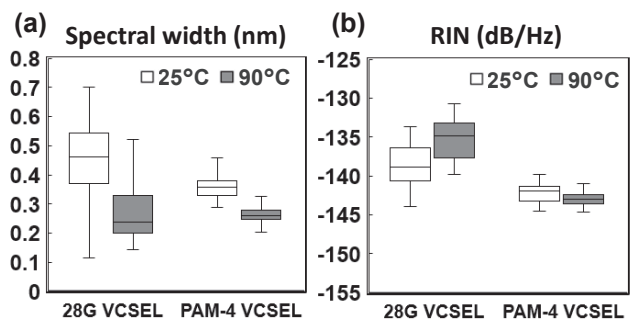

Fig. 10. Uniformity of spectral width (a) and RIN (b)

teristics, verifying that our array products have an adequate quality for 400 Gbit/s applications.

4. Conclusion

In this work, we have developed 850 nm/900 nm PAM-4 VCSEL arrays demanded for 400 Gbit/s short-reach communication. To achieve high-quality optical output waveform in PAM-4 modulation, we enhanced the optical confinement by tuning the epitaxial layer structure to a higher bandwidth, and optimized the shape of oxide aperture to reduce the RIN. We obtained a 3 dB bandwidth over 17 GHz even at high temperature, and succeeded in reducing the RIN by about 4 dB/Hz. These improvements leaded to excellent eye-patterns in the PAM-4 optical output waveform, for both the 850 nm/900 nm VCSELs. The uniformity of spectral width and RIN were improved by stabilizing the transverse mode, which is important for array products. These PAM-4 VCSEL arrays have enough performance and quality for 400 Gbit/s short-reach communication.

Technical Terms

*1 PAM-4: PAM-4 is a modulation format of signal based on four-level pulse amplitude modulation (PAM). It can transmit twice as much information as the conventional modulation format using two levels (on/off) such as NRZ.

*2 RIN: RIN is an abbreviation for relative intensity noise. It is the intensity fluctuations of light output power of a semiconductor laser normalized by the average output power.

*3 Relaxation oscillation frequency (f_r): Relaxation oscillation frequency is the characteristic frequency value at which optical frequency response starts to decrease rapidly. It dominates the modulation bandwidth of a semiconductor laser.

*4 TDECQ: TDECQ is an abbreviation for transmitter and dispersion eye closure for PAM-4. It is one of the figure-of-merits for PAM-4 waveform evaluation.

References

(1) IEEE P802.3cm, "400 Gb/s over Multimode Fiber Task Force," http://www.ieee802.org/3/cm/public/index.html

(2) "QSFP-DD MSA," http://www.qsfp-dd.com/

(3) "400G BiDi MSA," https://www.400gbidi-msa.org/

(4) S. E. Ralph, "Requirements and Results for Practical VCSEL Transmission using PAM-4 over MMF," 2016 Optical Fiber Communication Conference and Exhibition, Anaheim (USA), Mar. 2016, Tu2G.4

(5) R. Murty, "RMS Spectral Width," IEEE 802.3 400 Gb/s over Multimode Fiber Task Force (Jan. 2019)

(6) Chuan XIE, et al., "850 nm VCSEL and PD for Ultra High Speed Data Communication over Multimode Fiber," SEI Technical Review, No. 77 (October 2013)

(7) L. Coldren and S. Corzine, "Diode Lasers and Photonic Integrated Circuits," New York Wiley (1995)

(8) E. P. Haglund, et al., "Impact of Damping on Large Signal VCSEL Dynamics," International Semiconductor Laser Conference (ISLC), 7-10 (Sept. 2014)

(9) J. Lavrencik, et al., "Optimum VCSEL Apertures for High-Speed Multimode Fiber Links," Optical Fiber Communication Conference and Exhibition, M1I.1, San Diego (USA) (Mar. 2018)

(10) R. Kubota, et al., "850/900-nm VCSEL Arrays for 400 Gbit/s BiDi Applications," 24th OptoElectronics and Communications Conference (OECC) and 2019 International Conference on Photonics in Switching and Computing (PSC), Fukuoka (July 2019)

(11) T. Yoshikawa, et al., "Complete polarization control of 8×8 vertical-cavity surface-emitting laser matrix arrays," Appl. Phys. Lett. 66, 908 (1995)

(12) J. A. Tatum, et al., "VCSEL-Based Optical Transceivers for Future Data Center Applications," Optical Fiber Communication Conference and Exhibition, M3F.6, San Diego (USA) (Mar. 2018)

(13) J. Ingham, "Baseline proposal for a 400 Gb/s optical PMD supporting four MMF pairs," IEEE P802.3cm 400 Gb/s over Multimode Fiber Task Force (July 2018)

Contributors   The lead author is indicated by an asterisk (*).

T. AOKI*
- Ph.D.
  Assistant Manager, Transmission Devices Laboratory

R. KUBOTA
- Ph.D.
  Assistant Manager, Transmission Devices Laboratory

S. YOSHIMOTO
- Assistant General Manager, Transmission Devices Laboratory

M. YANAGISAWA
- Ph.D.
  Assistant General Manager, Transmission Devices Laboratory

T. ISHIZUKA
- Ph.D.
  Group Manager, Transmission Devices Laboratory

H. SHOJI
- Ph.D.
  Department Manager, Transmission Devices Laboratory